

C/EBP $\beta^{\Delta uORF}$ mice—a genetic model for uORF-mediated translational control in mammals

Klaus Wethmar,^{1,2} Valérie Bégay,^{1,5}
 Jeske J. Smink,^{1,5} Katrin Zaragoza,^{1,5}
 Volker Wiesenthal,^{1,6} Bernd Dörken,²
 Cornelis F. Calkhoven,³ and Achim Leutz^{1,4,7}

¹Max Delbrück Center for Molecular Medicine, D-13092 Berlin, Germany; ²Charité, Campus Virchow Klinikum, University Medicine Berlin, D-13353 Berlin, Germany; ³Leibniz Institute for Age Research—Fritz Lipmann Institute, D-07745 Jena, Germany; ⁴Department of Biology, Humboldt-University, D-10115 Berlin, Germany

Upstream ORFs (uORFs) are translational control elements found predominantly in transcripts of key regulatory genes. No mammalian genetic model exists to experimentally validate the physiological relevance of uORF-regulated translation initiation. We report that mice deficient for the CCAAT/enhancer-binding protein β (C/EBP β) uORF initiation codon fail to initiate translation of the autoantagonistic LIP (liver inhibitory protein) C/EBP β isoform. C/EBP $\beta^{\Delta uORF}$ mice show hyperactivation of acute-phase response genes, persistent repression of E2F-regulated genes, delayed and blunted S-phase entry of hepatocytes after partial hepatectomy, and impaired osteoclast differentiation. These data and the widespread prevalence of uORFs in mammalian transcriptomes suggest a comprehensive role of uORF-regulated translation in (patho)physiology.

Supplemental material is available at <http://www.genesdev.org>.

Received May 11, 2009; revised version accepted October 30, 2009.

Translational *cis*-regulatory upstream ORFs (uORFs) are found in the 5' mRNA regions of numerous eukaryotic transcripts and are considered to regulate protein expression by controlling translation reinitiation at downstream initiation codons or by activating the nonsense-mediated mRNA decay pathway (Morris and Geballe 2000). The frequency of conserved uORFs (Iacono et al. 2005; Calvo et al. 2009) and their predominant prevalence in transcripts of key regulatory genes of growth, differentiation, and proliferation (Kozak 1987) suggest an impor-

tant function of uORF-mediated translational control in mammals. Nevertheless, an experimental genetic model to examine the physiological relevance of uORF-regulated translation has not been established.

The transcription factor CCAAT/enhancer-binding protein β (C/EBP β) exerts important functions in many physiological processes, including metabolism, innate immunity, liver development, and regeneration (Tanaka et al. 1995; Greenbaum et al. 1998; Ramji and Foka 2002). The C/EBP β gene lacks introns, yet three N-terminal different isoforms (termed LAP* [liver-activating protein*], LAP, and LIP [liver inhibitory protein]) are translated from three consecutive in-frame AUG codons in a single transcript (Fig. 1A; Descombes and Schibler 1991). The truncated isoform LIP is devoid of N-terminal *trans*-activating domains but retains DNA-binding capacity and acts as a competitive inhibitor of the LAP and LAP* isoforms. Previous mutational analysis and tissue culture experiments suggested that translation of the conserved out-of-frame C/EBP β uORF restrains initiation of LAP and causes resumption of ribosomal scanning and reinitiation at the downstream LIP start site (Fig. 1B; Raught et al. 1996; Lincoln et al. 1998; Calkhoven et al. 2000).

Results and Discussion

To determine the physiological importance of uORF-mediated translational control, recombinant mice were generated by introduction of an ATG-to-TTG point mutation at the C/EBP β uORF translational initiation site (Fig. 1B; Supplemental Fig. S2). The C/EBP $\beta^{\Delta uORF}$ mutation was designed to abrogate uORF initiation without altering the amino acid sequence of C/EBP β . A C/EBP β wild-type knock-in control strain (C/EBP β^{WT}) was generated and analyzed in parallel to exclude potential artifacts caused by the gene targeting approach. Throughout the experiments, no differences were detected between C/EBP β^{WT} and parental wild-type mice. Offspring of heterozygous C/EBP $\beta^{\Delta uORF}$ matings showed the expected Mendelian ratio (Supplemental Table S1). Homozygous C/EBP $\beta^{\Delta uORF}$ mice showed normal weight gain and no overt developmental defects or premature death (Supplemental Fig. S3). In contrast to C/EBP β knockout animals, homozygous C/EBP $\beta^{\Delta uORF}$ females were fertile, gave birth to normal size litters (eight out of eight females tested), and showed intact mammary gland development and function (Robinson et al. 1998; Seagroves et al. 1998; Supplemental Figs. S3A, S4).

Bacterial lipopolysaccharide (LPS) is a major inducer of acute-phase response mediated by C/EBP β in the liver (Poli 1998), and has been shown to enhance expression of the truncated C/EBP β isoform LIP (Timchenko et al. 2005). In livers of C/EBP β^{WT} mice, LIP was strongly induced after LPS administration, whereas C/EBP $\beta^{\Delta uORF}$ mice failed to express high levels of LIP (Fig. 1C). Likewise, lung, spleen, and white adipose tissue of C/EBP $\beta^{\Delta uORF}$ mice displayed reduced expression of LIP after LPS treatment as compared with C/EBP β^{WT} tissues (Supplemental Fig. S5). Failure to induce LIP was also observed in C/EBP $\beta^{\Delta uORF}$ mouse embryo fibroblasts (MEFs) (Fig. 1D) and was associated with superactivation of a C/EBP-responsive luciferase reporter (Fig. 1E), suggesting a lack of *trans*-repressive function of LIP. Hence, genetic ablation

[*Keywords*: Upstream ORF; translational control; C/EBP β ; liver regeneration; cell cycle]

⁵These authors contributed equally to this work.

⁶Present address: Deutsches Zentrum für Luft- und Raumfahrt e.V., Heinrich-Konen-Str. 1, 53227 Bonn, Germany.

⁷Corresponding author.

E-MAIL aleutz@mdc-berlin.de; FAX 49-30-9406-3298.

Article is online at <http://www.genesdev.org/cgi/doi/10.1101/gad.557910>. Freely available online through the *Genes & Development* Open Access option.

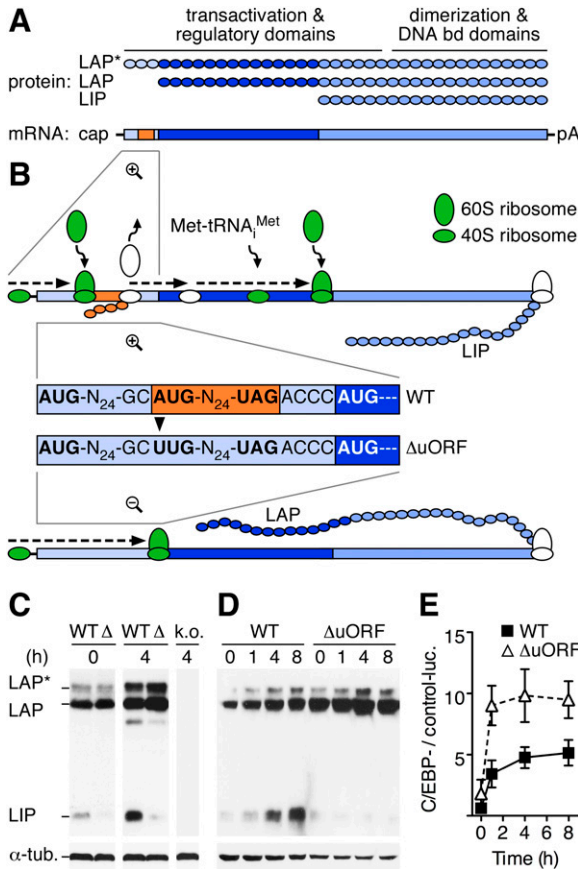


Figure 1. Genetic ablation of *cis*-regulatory translational control by the C/EBPβ uORF. (A) Three protein isoforms (LAP* [38 kDa], LAP [35 kDa], and LIP [20 kDa]) are translated from consecutive in-frame initiation codons in the same transcript (Descombes and Schibler 1991). The C/EBPβ mRNA contains a conserved *cis*-regulatory small uORF (30 base pairs [bp], orange) terminating 4 bp upstream of the LAP initiation site in a different reading frame. (bd) Binding; (pA) poly(A) tail. (B) Translation of the uORF serves to strip ribosomes from their initiating Met-tRNA_{Met} (green to white) and prevents initiation at the proximate LAP initiation codon. Upon reloading of ribosomes with the ternary eIF2-GTP-Met-tRNA_{Met} complex (white to green), translation reinitiation from the downstream AUG codon generates LIP. In C/EBPβ^{ΔuORF} mice, an A-to-U point mutation was designed to abrogate ribosomal initiation at the uORF start codon without changing the amino acid sequence of the C/EBPβ isoforms. Most ribosomes will thus initiate at the LAP AUG instead. (Display of LAP* translation was omitted for simplicity. For details on alternative start site selection, see Supplemental Fig. S1.) (C) Upon i.p. injection of LPS, LIP is strongly induced in C/EBPβ^{WT} (WT) but not in C/EBPβ^{ΔuORF} livers (Δ). (h) Hours of LPS treatment; (α-tub.) α-tubulin; (k.o.) lysate of C/EBPβ knockout mouse. (D) In MEFs, LPS induces LIP expression in C/EBPβ^{WT} but not in C/EBPβ^{ΔuORF} cells. (E) Representative luciferase reporter assay (*n* = 3) demonstrating increased luciferase reporter activity (luc.) in C/EBPβ^{ΔuORF} (open triangles) as compared with C/EBPβ^{WT} (black squares) MEFs at indicated times after LPS treatment. Error bars show SEM.

of the C/EBPβ uORF in mice abolishes the inducible expression of LIP and validates the functional importance of the C/EBPβ uORF as a translational *cis*-regulatory element in the animal.

Recently, we showed that the long and truncated C/EBPβ isoforms opposingly regulate the differentiation of bone-resorbing osteoclasts (Smink et al. 2009). C/EBPβ^{LIP} mice that express LIP only and not the long C/EBPβ

isoforms showed strongly enhanced osteoclast differentiation. Ectopic expression of LAP inhibited osteoclast differentiation (Smink et al. 2009), suggesting that an increase of the LAP/LIP isoform ratio in C/EBPβ^{ΔuORF} mice would also inhibit osteoclastogenesis. In tibiae of C/EBPβ^{ΔuORF} mice, we observed a reduction in osteoclast size and number (Fig. 2A), which was accompanied by an increase in thickness of bone trabeculae and bone volume (Supplemental Fig. S6). Bone marrow cell cultures from C/EBPβ^{ΔuORF} mice formed fewer and smaller osteoclasts as compared with C/EBPβ^{WT} and failed to express LIP (Fig. 2B,C). C/EBPβ^{ΔuORF} osteoclasts showed increased expression of the transcription factor MafB (Fig. 2D), a previously identified target of LAP and a repressor of osteoclastogenesis (Smink et al. 2009). MafB inhibits a number of osteoclastic genes, including *Nfatc1*, *Oscar*, *Atp6v0d2*, *DC-STAMP*, and *TRACP* (Kim et al. 2007, 2008; Smink et al. 2009). Transcript levels of these osteoclast markers were found to be reduced in C/EBPβ^{ΔuORF} osteoclasts (Fig. 2E), while expression of the MafB-independent *c-Fos* gene (Kim et al. 2007) was not affected. These data suggest that the abrogation of C/EBPβ uORF-mediated translational control, and the

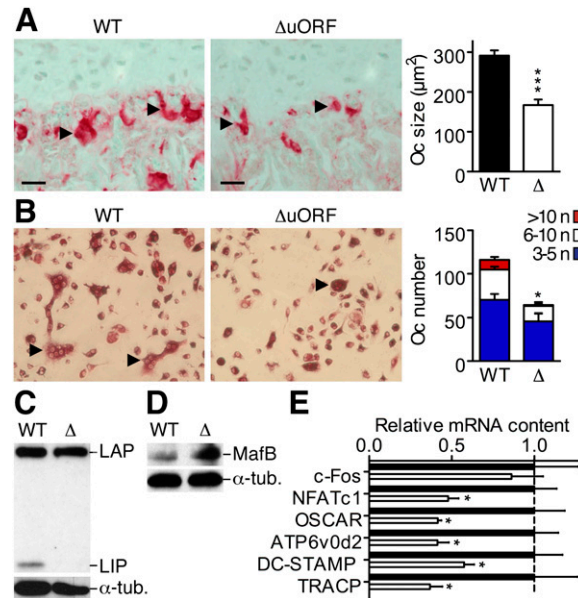


Figure 2. The C/EBPβ^{ΔuORF} mutation impairs osteoclast differentiation. (A) Tibia sections showing tartrate-resistant acid phosphatase (TRACP)-stained osteoclasts (red staining, light-green counterstain) in C/EBPβ^{ΔuORF} as compared with C/EBPβ^{WT} mice. (Arrowheads) Multinucleated osteoclasts; bars, 50 μm. The bar graph displays average osteoclast sizes as determined from six mice per genotype at 8 wk of age. (B) TRACP staining (red) showing osteoclast differentiation of bone marrow-derived precursors of C/EBPβ^{ΔuORF} and C/EBPβ^{WT} mice after 6 d in culture with M-CSF and RANK-L (*n* = 6). (Arrowheads) Multinucleated osteoclasts. The bar graph displays the differential quantification of osteoclasts by the number of nuclei (*n*) per cell. (C) Immunoblot analysis showing LIP expression in C/EBPβ^{WT} but not in C/EBPβ^{ΔuORF} osteoclasts at day 2 of culture. (D) Immunoblot analysis showing increased MafB protein in C/EBPβ^{ΔuORF} as compared with C/EBPβ^{WT} osteoclasts. (E) Real-time PCR analysis showing decreased expression of MafB-regulated osteoclast markers in C/EBPβ^{ΔuORF} (open bars) as compared with C/EBPβ^{WT} (black bars) osteoclasts. Normalized to Gapdh (glyceraldehyde-3-phosphate-dehydrogenase) and presented relative to C/EBPβ^{WT} (set to 1, dashed line). Error bars show SEM; (*) *P* < 0.05; (***) *P* < 0.001.

resulting increase in the LAP/LIP ratio, constrains osteoclast differentiation by enhancing the expression of MafB.

Since C/EBPβ is an important regulator of liver regeneration, acute-phase response, and interleukin-6 (IL-6) expression (Screpanti et al. 1995; Greenbaum et al. 1998; Poli 1998), we implemented partial hepatectomy (PH) to analyze the consequences of the C/EBPβ^{ΔuORF} mutation in this physiological context. C/EBPβ^{ΔuORF} mice failed to induce expression of the truncated LIP isoform throughout the 72-h observation period after PH (Fig. 3A), while LIP was strongly induced in a two-wave kinetic in regenerating livers of C/EBPβ^{WT} animals, suggesting consecutive functions of LIP in the course of liver regeneration. After PH, IL-6 serum levels of C/EBPβ^{ΔuORF} mice rose higher as compared with control animals (Fig. 3B), reaching a 4.7-fold difference after 3 h (1254 ± 265 vs. 263 ± 49 pg/mL, *n* = 6, *P* < 0.01) and a 3.3-fold difference at the peak of wild-type expression 6 h after surgery (1578 ± 132 vs. 472 ± 93 pg/mL, *n* = 6, *P* < 0.01). IL-6 signaling is known to rapidly confer activating phosphomodifications to both C/EBPβ and STAT3 transcription factors (Akira 1997), resulting in synergistic induction of type I acute-phase response genes (Alonzi et al. 2001). Real-time PCR analysis of known acute-phase response C/EBPβ target genes revealed consistently increased transcription of *serum amyloid A1* (*Saa1*), *α-1 antitrypsin* (*Aat*), *haptoglobin* (*Hp*), and *hemopexin* (*Hpx*), ranging from 1.2-fold to 8.0-fold in hepatectomized C/EBPβ^{ΔuORF} as compared with C/EBPβ^{WT} mice (Fig. 3C). Maxima of en-

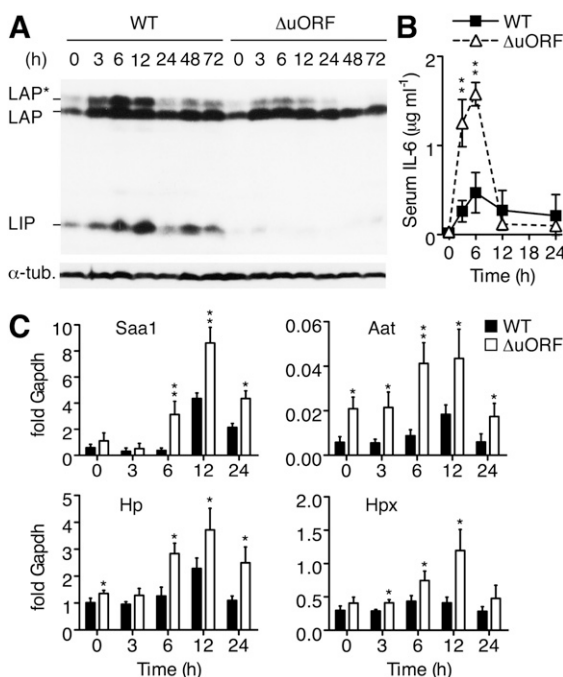


Figure 3. The C/EBPβ^{ΔuORF} mutation causes superinduction of C/EBPβ target genes. (A) Induction of LIP in C/EBPβ^{WT} livers upon PH is abolished in C/EBPβ^{ΔuORF} animals. (B) ELISA showing elevated average levels of serum IL-6 at 3 h and 6 h after PH in C/EBPβ^{ΔuORF} (open triangles) as compared with C/EBPβ^{WT} (black squares) animals (*n* = 6; **** *P* < 0.01). (C) Real-time PCR analysis demonstrating elevated mRNA contents of acute-phase response genes in C/EBPβ^{ΔuORF} (open bars) as compared with C/EBPβ^{WT} (black bars) livers at indicated times after PH (*n* = 6; *** *P* < 0.05; **** *P* < 0.01). Error bars show SEM.

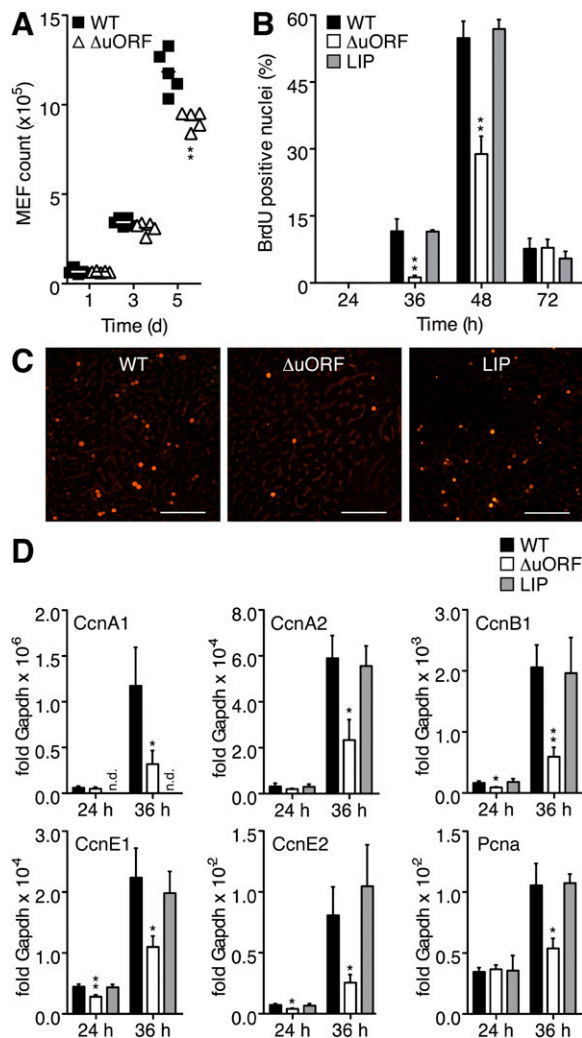


Figure 4. Cell proliferation defect in C/EBPβ^{ΔuORF} mice. (A) *In vitro* proliferation assay demonstrating reduced expansion of C/EBPβ^{ΔuORF} (open triangles) as compared with C/EBPβ^{WT} (black squares) MEF cultures (*n* = 5 independent embryos per genotype; **** *P* < 0.01). (B) Quantification of BrdU-labeled hepatocyte nuclei (2-h pulse-labeling) in liver sections showing a reduced proportion of hepatocytes in S phase in C/EBPβ^{ΔuORF} (open bars) as compared with C/EBPβ^{WT} (black bars) and C/EBPβ^{LIP} (gray bars) livers at 36 and 48 h after PH (*n* = 8, ***** *P* < 0.001; *n* = 7, *** *P* < 0.05 vs. wild type, respectively). (C) BrdU immunofluorescence stainings of C/EBPβ^{WT}, C/EBPβ^{ΔuORF}, and C/EBPβ^{LIP} liver sections 36 h after PH. Bars, 100 μm. (D) Real-time PCR analysis showing reduced mRNA contents of *CcnA1*, *CcnA2*, *CcnB1*, *CcnE1*, *CcnE2*, and *PcnA* in C/EBPβ^{ΔuORF} (open bars) as compared with C/EBPβ^{WT} (black bars) and C/EBPβ^{LIP} (gray bars) livers at indicated times after PH. (*n* = 6, *** *P* < 0.05, **** *P* < 0.01 vs. wild type). (n.d.) Not determined. Error bars show SEM.

hanced expression of *Saa1*, *Aat*, and *Hp* in C/EBPβ^{ΔuORF} mice correlated with the peak of LAP expression at 6 h after surgery (Fig. 3A). Together with the superactivation of the C/EBP-responsive reporter construct in C/EBPβ^{ΔuORF} MEFs, these data suggest that uORF-mediated induction of LIP serves to restrict the *trans*-activation of early acute-phase response genes.

In an *in vitro* proliferation assay, reduced expansion of C/EBPβ^{ΔuORF} MEF cultures became evident at day 3 (Fig. 4A) and resulted in significantly lower cell numbers at

day 5 of the experiment (9.2 ± 0.2 vs. $11.9 \pm 0.5 \times 10^5$ per well, $n = 5$, $P < 0.01$) as compared with C/EBP β^{WT} MEFs. To examine whether the C/EBP $\beta^{\Delta\text{uORF}}$ mutation also affected cell proliferation in mice, we compared liver regeneration properties of C/EBP $\beta^{\Delta\text{uORF}}$, C/EBP β^{WT} , and C/EBP β^{LIP} animals (C/EBP β expression control in Supplemental Fig. S7). Hepatocytes in regenerating livers of C/EBP $\beta^{\Delta\text{uORF}}$ mice entered the cell cycle later and at lower frequency as compared with C/EBP β^{WT} animals (Fig. 4B,C). S-phase labeling of liver cells by 5-Bromo-2-deoxyuridine (BrdU) revealed a 9.3-fold reduction in the proportion of BrdU-positive C/EBP $\beta^{\Delta\text{uORF}}$ hepatocytes at 36 h ($1.2\% \pm 0.5\%$ vs. $11.6\% \pm 2.8\%$, $n = 8$, $P < 0.01$) and a 1.9-fold reduction at 48 h after surgery ($28.9\% \pm 4.0\%$ vs. $54.9\% \pm 3.8\%$, $n = 7$, $P < 0.01$). At the same times, regenerating C/EBP β^{LIP} livers contained similar numbers of BrdU-positive hepatocytes as compared with C/EBP β^{WT} (36 h: $11.5\% \pm 0.4\%$, $n = 5$; 48 h: $56.9\% \pm 2.1\%$, $n = 4$). Virtually no BrdU incorporation was observed in hepatocytes of sham-operated animals at 48 h after PH ($n = 3$) (data not shown). Transcript levels of cyclin A1 (CcnA1), CcnA2, CcnB1, CcnE1, CcnE2, and proliferating cell nuclear antigen (Pcna) were induced at 36 h after PH in C/EBP β^{WT} and C/EBP β^{LIP} livers, but remained significantly lower in C/EBP $\beta^{\Delta\text{uORF}}$ animals (Fig. 4D). Twelve hours later, the expression of the cyclins and Pcna were similar in the three genotypes (data not shown), suggesting that re-entry of C/EBP $\beta^{\Delta\text{uORF}}$ hepatocytes into the cell cycle was impaired but not abolished by the compromised induction of LIP. Similar recovery of liver weight in C/EBP β^{WT} and C/EBP $\beta^{\Delta\text{uORF}}$ mice, accompanied by an increased hepatocyte volume in C/EBP $\beta^{\Delta\text{uORF}}$ livers (Supplemental Fig. S8), suggested that enhanced hepatocyte hypertrophy compensated for the blunted S-phase entry to restore adequate liver/body weight ratios.

To further characterize the altered dynamics of cell cycle entry in regenerating C/EBP $\beta^{\Delta\text{uORF}}$ livers, we performed a genome-wide microarray expression analysis at 36 h after PH. A total number of 546 underrepresented transcripts (392 annotated genes) and 266 overrepresented transcripts (161 annotated genes) were identified in regenerating C/EBP $\beta^{\Delta\text{uORF}}$ as compared with C/EBP β^{WT} livers (Fig. 5A; Supplemental Table S2). Comparison of all deregulated

transcripts to a database of cell cycle-associated genes (<http://www.geneontology.org>) resulted in 191 matches, of which 99% (189 matches) grouped to the underrepresented fraction (Fig. 5A; Supplemental Table S3). The microarray analysis results were validated for a selection of transcripts on the mRNA (Fig. 4D) and/or the protein level (Supplemental Fig. S9). The high proportion of underrepresented cell cycle genes at 36 h after PH verified the immunohistochemically detected reduction in hepatocyte S-phase entry in C/EBP $\beta^{\Delta\text{uORF}}$ mice on a transcriptional level, and implied a regulatory function of the C/EBP β LAP/LIP isoform ratio.

C/EBP transcription factors are known to affect the expression of cell cycle regulatory genes controlled by E2F transcription factors (Sebastian and Johnson 2006; Nerlov 2007). Full-length C/EBP α (p42), but not the N-terminally truncated isoform (p30), acts as a cell cycle inhibitor by repressing E2F target genes (Slomiany et al. 2000; Porse et al. 2001; Iakova et al. 2003). For C/EBP β , isoform-specific data on E2F coregulation is scarce and suggested a corepressive function of LAP (Sebastian et al. 2005). A comparison of deregulated cell cycle genes in regenerating C/EBP $\beta^{\Delta\text{uORF}}$ liver to previously identified E2F targets (Ishida et al. 2001; Ren et al. 2002; Bracken et al. 2004) revealed that at least 42% of them were known E2F target genes. Chromatin immunoprecipitation (ChIP) analysis performed 36 h after PH showed that both E2F3 and C/EBP β were associated with promoters of underrepresented E2F target genes in regenerating liver (*E2F1*, *Rb1* [*retinoblastoma-like 1*], *CcnA2*, *CcnE1*, *Cdc2* [*cell division cycle-associated 2*], *Cdc25*, *Mcm3* [*minichromosome maintenance-deficient 3*], *Mcm6*, and *Plk1* [*Polo-like kinase 1*]) (Fig. 5B). At the same time, C/EBP α showed little or no association with these E2F target gene promoters. Furthermore, transient down-regulation of transcript and protein levels of C/EBP α after PH (Supplemental Fig. S10) suggested a predominant role for C/EBP β in the coregulation of many E2F target genes in cycling hepatocytes. To examine the effect of individual C/EBP β isoforms on E2F coregulation, we used an E2F-responsive luciferase reporter construct that has been employed previously to address the mechanism of C/EBP-mediated E2F repression (Porse et al. 2001). Luciferase activity induced by ectopic expression of

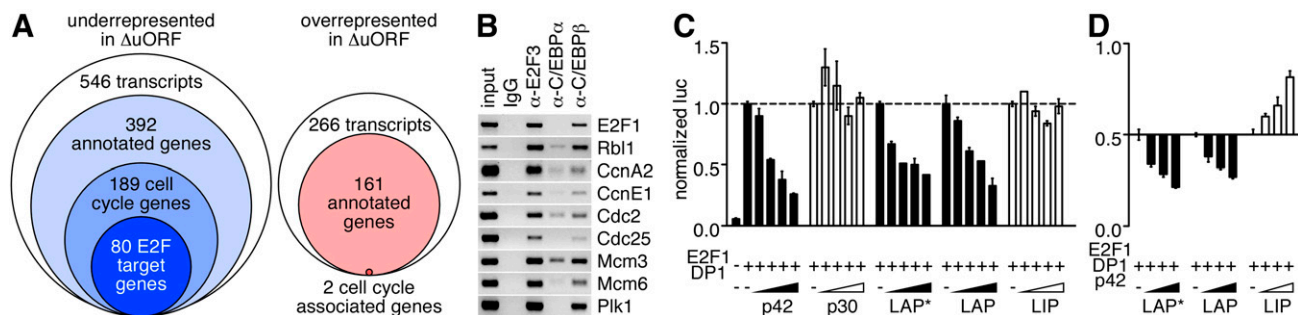


Figure 5. The C/EBP $\beta^{\Delta\text{uORF}}$ mutation causes repression of E2F target genes. (A) Graphic representation of a genome-wide microarray expression analysis comparing transcript levels in C/EBP β^{WT} and C/EBP $\beta^{\Delta\text{uORF}}$ liver at 36 h after PH. (B) Representative ChIP assay on C/EBP $\beta^{\Delta\text{uORF}}$ liver chromatin showing the association of E2F3, C/EBP α , and C/EBP β to indicated gene promoters in regenerating liver at 36 h after PH ($n = 2$). (C) Luciferase reporter assay demonstrating the repressive function of long (black bars), but not of truncated (open bars) C/EBP α and C/EBP β isoforms on the pGL3TATAbasic-6x E2F reporter construct ($n = 3$). (luc) Luciferase activity; (p42 and p30) long and truncated C/EBP α isoforms. (D) Luciferase reporter assay with constant, intermediately repressive C/EBP α p42 expression (luciferase activity set to 0.5) showing the corepressive function of LAP* and LAP (black bars) and the derepressive function of LIP (open bars) on the same E2F-responsive reporter construct as used in C ($n = 3$). Error bars show SEM.

the transcription factors E2F1 and DP1 (dimerization partner 1, conferring full activity to E2F1) was proportionally repressed by increasing amounts of coexpressed p42, LAP*, or LAP, but remained unaffected by coexpression of p30 or LIP (Fig. 5C). Importantly, the inhibition of E2F activity by p42 was effectively relieved by coexpression of LIP, whereas increasing amounts of LAP* or LAP further repressed reporter activity (Fig. 5D).

Liver regeneration defects observed in C/EBP β knockout mice have been attributed to a lack of coactivating C/EBP β function on E2F target genes (Greenbaum et al. 1998; Wang et al. 2007). This interpretation contrasts data showing E2F-repressive functions of LAP in vitro (Sebastian et al. 2005) and LAP-mediated retardation of hepatocyte cell cycle entry after PH in mice (Luedde et al. 2004). Our observations of impaired cell cycle entry in C/EBP $\beta^{\Delta uORF}$ livers and the rescue of this phenotype in C/EBP β^{LIP} mice suggest that long C/EBP β isoforms are dispensable for accurate hepatocyte S-phase entry. The data presented here imply a model in which uORF-mediated induction of LIP is required to overcome repression of E2F targets by long C/EBP α and C/EBP β isoforms to facilitate rapid cell cycle entry during liver regeneration.

The analysis of the C/EBP $\beta^{\Delta uORF}$ mice proves the physiological relevance of uORF-mediated translational control in mammals. We note that low amounts of LIP can be detected in C/EBP $\beta^{\Delta uORF}$ mice, which might originate from leaky ribosomal scanning over both the LAP* and LAP start codons (Supplemental Fig. S1) or from partial proteolytic cleavage (Baer and Johnson 2000). Nevertheless, the lack of a functional C/EBP β uORF start codon results in the inability to induce LIP expression under inflammatory conditions, as well as during differentiation and regeneration processes. Aberrant protein expression caused by defective translational control is increasingly recognized as a pathophysiological mechanism in the etiology of human diseases (Scheper et al. 2007). Specifically, mutations affecting uORF-mediated translational control have been connected to the development of diseases such as hereditary thrombocythemia (Wiestner et al. 1998), familial cutaneous melanoma (Liu et al. 1999), or Marie Unna hereditary hypotrichosis (Wen et al. 2009). The high prevalence of uORFs in human transcripts (35%–49%) implies a comprehensive, yet underestimated, *cis*-regulatory function in adjusting protein expression (Iacono et al. 2005; Calvo et al. 2009). Future studies will have to address to what extent aberrant uORF-mediated translational control accounts for the development of disease, and how it can be targeted by therapeutic intervention.

Materials and methods

Generation of C/EBP $\beta^{\Delta uORF}$ and C/EBP β^{WT} mice

Mutant (C/EBP $\beta^{\Delta uORF}$) and control (C/EBP β^{WT}) mice were generated by homologous recombination according to standard protocols (Supplemental Fig. S2). The neomycin cassette was removed by crossing C/EBP $\beta^{\Delta uORF}$ and C/EBP β^{WT} mice to the Cre-deleter strain (Schwenk et al. 1995), and the new strains were kept in a 129Ola \times C57Bl/6 background. Female and male mice showed the same phenotype and were analyzed as one group. Mice were provided with standard mouse diet and water ad libitum on a 12-h light–dark cycle. All procedures and animal experiments were conducted in compliance with protocols approved by the Institutional Animal Care and Use Committee.

Additional methods can be found in the Supplemental Material.

Acknowledgments

We thank C. Birchmeier for providing the pTV-flox targeting vector; K. Helin, S. Gaubatz, and E. Kowenz-Leutz for kind donation of luciferase reporter or expression plasmids; J. Lausen and O. Pless for continuous scientific discussion; M. Borowiak, B. von Eyss, and U. Ziebold for valuable technical advice; M. Huska and M. Andrade for help with microarray data analysis; and N. Burbach, R. Zarmstorff, and S. Schmidt for excellent assistance. This work was supported by the Deutsche Krebsstiftung (grant 107968 to K.W. and A.L.).

References

- Akira S. 1997. IL-6-regulated transcription factors. *Int J Biochem Cell Biol* **29**: 1401–1418.
- Alonzi T, Maritano D, Gorgoni B, Rizzuto G, Libert C, Poli V. 2001. Essential role of STAT3 in the control of the acute-phase response as revealed by inducible gene activation in the liver. *Mol Cell Biol* **21**: 1621–1632.
- Baer M, Johnson PF. 2000. Generation of truncated C/EBP β isoforms by in vitro proteolysis. *J Biol Chem* **275**: 26582–26590.
- Bracken AP, Ciro M, Cocito A, Helin K. 2004. E2F target genes: Unravels the biology. *Trends Biochem Sci* **29**: 409–417.
- Calkhoven CF, Muller C, Leutz A. 2000. Translational control of C/EBP α and C/EBP β isoform expression. *Genes & Dev* **14**: 1920–1932.
- Calvo SE, Pagliarini DJ, Mootha VK. 2009. Upstream open reading frames cause widespread reduction of protein expression and are polymorphic among humans. *Proc Natl Acad Sci* **106**: 7507–7512.
- Descombes P, Schibler U. 1991. A liver-enriched transcriptional activator protein, LAP, and a transcriptional inhibitory protein, LIP, are translated from the same mRNA. *Cell* **67**: 569–579.
- Greenbaum LE, Li W, Cressman DE, Peng Y, Ciliberto G, Poli V, Taub R. 1998. CCAAT enhancer-binding protein β is required for normal hepatocyte proliferation in mice after partial hepatectomy. *J Clin Invest* **102**: 996–1007.
- Iacono M, Mignone F, Pesole G. 2005. uAUG and uORFs in human and rodent 5' untranslated mRNAs. *Gene* **349**: 97–105.
- Iakova P, Awad SS, Timchenko NA. 2003. Aging reduces proliferative capacities of liver by switching pathways of C/EBP α growth arrest. *Cell* **113**: 495–506.
- Ishida S, Huang E, Zuzan H, Spang R, Leone G, West M, Nevins JR. 2001. Role for E2F in control of both DNA replication and mitotic functions as revealed from DNA microarray analysis. *Mol Cell Biol* **21**: 4684–4699.
- Kim K, Kim JH, Lee J, Jin HM, Kook H, Kim KK, Lee SY, Kim N. 2007. MafB negatively regulates RANKL-mediated osteoclast differentiation. *Blood* **109**: 3253–3259.
- Kim K, Lee SH, Ha Kim J, Choi Y, Kim N. 2008. NFATc1 induces osteoclast fusion via up-regulation of Atp6v0d2 and the dendritic cell-specific transmembrane protein (DC-STAMP). *Mol Endocrinol* **22**: 176–185.
- Kozak M. 1987. An analysis of 5'-noncoding sequences from 699 vertebrate messenger RNAs. *Nucleic Acids Res* **15**: 8125–8148.
- Lincoln AJ, Monczak Y, Williams SC, Johnson PF. 1998. Inhibition of CCAAT/enhancer-binding protein α and β translation by upstream open reading frames. *J Biol Chem* **273**: 9552–9560.
- Liu L, Dilworth D, Gao L, Monzon J, Summers A, Lassam N, Hogg D. 1999. Mutation of the CDKN2A 5' UTR creates an aberrant initiation codon and predisposes to melanoma. *Nat Genet* **21**: 128–132.
- Luedde T, Duderstadt M, Streetz KL, Tacke F, Kubicka S, Manns MP, Trautwein C. 2004. C/EBP β isoforms LIP and LAP modulate progression of the cell cycle in the regenerating mouse liver. *Hepatology* **40**: 356–365.
- Morris DR, Geballe AP. 2000. Upstream open reading frames as regulators of mRNA translation. *Mol Cell Biol* **20**: 8635–8642.
- Nerlov C. 2007. The C/EBP family of transcription factors: A paradigm for interaction between gene expression and proliferation control. *Trends Cell Biol* **17**: 318–324.
- Poli V. 1998. The role of C/EBP isoforms in the control of inflammatory and native immunity functions. *J Biol Chem* **273**: 29279–29282.
- Porse BT, Pedersen TA, Xu X, Lindberg B, Wewer UM, Friis-Hansen L, Nerlov C. 2001. E2F repression by C/EBP α is required for adipogenesis and granulopoiesis in vivo. *Cell* **107**: 247–258.

- Ramji DP, Foka P. 2002. CCAAT/enhancer-binding proteins: Structure, function and regulation. *Biochem J* **365**: 561–575.
- Raught B, Gingras AC, James A, Medina D, Sonenberg N, Rosen JM. 1996. Expression of a translationally regulated, dominant-negative CCAAT/enhancer-binding protein β isoform and up-regulation of the eukaryotic translation initiation factor 2α are correlated with neoplastic transformation of mammary epithelial cells. *Cancer Res* **56**: 4382–4386.
- Ren B, Cam H, Takahashi Y, Volkert T, Terragni J, Young RA, Dynlacht BD. 2002. E2F integrates cell cycle progression with DNA repair, replication, and G(2)/M checkpoints. *Genes & Dev* **16**: 245–256.
- Robinson GW, Johnson PF, Hennighausen L, Sterneck E. 1998. The C/EBP β transcription factor regulates epithelial cell proliferation and differentiation in the mammary gland. *Genes & Dev* **12**: 1907–1916.
- Scheper GC, van der Knaap MS, Proud CG. 2007. Translation matters: Protein synthesis defects in inherited disease. *Nat Rev Genet* **8**: 711–723.
- Schwenk F, Baron U, Rajewsky K. 1995. A cre-transgenic mouse strain for the ubiquitous deletion of loxP-flanked gene segments including deletion in germ cells. *Nucleic Acids Res* **23**: 5080–5081.
- Screpanti I, Romani L, Musiani P, Modesti A, Fattori E, Lazzaro D, Sellitto C, Scarpa S, Bellavia D, Lattanzio G, et al. 1995. Lymphoproliferative disorder and imbalanced T-helper response in C/EBP β -deficient mice. *EMBO J* **14**: 1932–1941.
- Seagroves TN, Krnacik S, Raught B, Gay J, Burgess-Beusse B, Darlington GJ, Rosen JM. 1998. C/EBP β , but not C/EBP α , is essential for ductal morphogenesis, lobuloalveolar proliferation, and functional differentiation in the mouse mammary gland. *Genes & Dev* **12**: 1917–1928.
- Sebastian T, Johnson PF. 2006. Stop and go: Anti-proliferative and mitogenic functions of the transcription factor C/EBP β . *Cell Cycle* **5**: 953–957.
- Sebastian T, Malik R, Thomas S, Sage J, Johnson PF. 2005. C/EBP β cooperates with RB:E2F to implement Ras(V12)-induced cellular senescence. *EMBO J* **24**: 3301–3312.
- Slomiany BA, D'Arigo KL, Kelly MM, Kurtz DT. 2000. C/EBP α inhibits cell growth via direct repression of E2F-DP-mediated transcription. *Mol Cell Biol* **20**: 5986–5997.
- Smink JJ, Begay V, Schoenmaker T, Sterneck E, de Vries TJ, Leutz A. 2009. Transcription factor C/EBP β isoform ratio regulates osteoclastogenesis through MafB. *EMBO J* **28**: 1769–1781.
- Tanaka T, Akira S, Yoshida K, Umemoto M, Yoneda Y, Shirafuji N, Fujiwara H, Suematsu S, Yoshida N, Kishimoto T. 1995. Targeted disruption of the NF-IL6 gene discloses its essential role in bacteria killing and tumor cytotoxicity by macrophages. *Cell* **80**: 353–361.
- Timchenko NA, Wang G-L, Timchenko LT. 2005. RNA CUG-binding Protein 1 increases translation of 20-kDa isoform of CCAAT/enhancer-binding protein β by interacting with the α and β subunits of eukaryotic initiation translation factor 2. *J Biol Chem* **280**: 20549–20557.
- Wang H, Larris B, Peiris TH, Zhang L, Le Lay J, Gao Y, Greenbaum L. 2007. C/EBP β activates E2F regulated genes in vivo via recruitment of the coactivator CBP/P300. *J Biol Chem* **282**: 24679–24688.
- Wen Y, Liu Y, Xu Y, Zhao Y, Hua R, Wang K, Sun M, Li Y, Yang S, Zhang XJ, et al. 2009. Loss-of-function mutations of an inhibitory upstream ORF in the human hairless transcript cause Marie Unna hereditary hypotrichosis. *Nat Genet* **41**: 228–233.
- Wiestner A, Schlemper RJ, van der Maas AP, Skoda RC. 1998. An activating splice donor mutation in the thrombopoietin gene causes hereditary thrombocythaemia. *Nat Genet* **18**: 49–52.